Available online at www.sciencedirect.com
ScienceDirect
Comparative Biochemistry and Physiology, Part A 150 (2008) 131–135
CBP
www.elsevier.com/locate/cbpa

Kinematics of Swimming Garter Snakes (*Thamnophis sirtalis*) ☆

Yonatan Munk *

Department of Integrative Biology, University of California, Berkeley, CA 94720, USA

Received 7 March 2006; received in revised form 10 August 2007; accepted 9 September 2007
Available online 14 September 2007

Abstract

We investigate the kinematics of swimming garter snakes (*Thamnophis sirtalis*) using a novel nonlinear regression-based digitization method to establish quantitative statistical support for non-constant wavelengths in the undulatory pattern exhibited by swimming snakes. We find that in swimming snakes, the growth of the amplitude of the propulsive wave head-to-tail is strongly correlated ($p<0.005$) with the head-to-tail growth in the wavelength. We investigate correlations between kinematic parameters and steady swimming speed, and find a very strong positive correlation between swimming speed and undulation frequency. We furthermore find a statistically well-supported positive correlation between swimming speed and both the initial amplitude of the propulsive wave at the head and the degree of amplitude growth from head to tail.

Keywords: Snakes; Swimming; Kinematics; Anguilliform; Locomotion; *Thamnophis sirtalis*

1. Introduction

The study of anguilliform swimming has a rich history and has benefited greatly from the attentions of such scientific luminaries as Sir James Gray, G.I. Taylor and Sir James Lighthill. As reviewed by Gillis (1996), the seminal work of Gray (1933) laid the groundwork for many subsequent studies of undulatory swimming kinematics including work by Hertel (1966), Lighthill (1975), Blake (1983), Jayne (1985), Graham et al. (1987), and Jordan (1996).

The study of swimming snakes has historically attracted interest due to the relative ease of performing hydrodynamic analyses on 'bad' hydromechanical shapes (Taylor, 1952; Lighthill, 1969, 1971). Early studies typically modeled the undulatory pattern exhibited by long and slender animals using a sinusoidal wave of constant wavelength and frequency, implying that the propulsive wave travels down the length of the body with constant speed. This has been shown to be a valid in many biological cases (e.g. eels (Gillis, 1998; Tytell and Lauder, 2004; Tytell, 2004b), saithe Videler and Hess (1984), etc.).

In some anguilliform swimmers, however, it has been observed that the wavelength of the propulsive wave increases from head to tail while maintaining constant frequency, implying an increasing propagation speed for the wave. Jayne (1985) observed this phenomenon first in his landmark study comparing swimming kinematics of a constricting colubrid snake species (*Elaphe g. guttata*) and a non-constricting colubrid snake species (*Nerodia fasciata pictiventris*). Graham et al. (1987) noted a similar pattern in the kinematics of swimming sea snakes (*Pelamis platurus*), as did Gillis (1997) for fully aquatic salamanders (*Siren intermedia*) swimming at high speeds. The bulk of the literature relating to anguilliform kinematics relates to steady swimming, although recently Tytell (2004a) has investigated the kinematics and hydrodynamics of linear accelerations in eels.

Previous methods of quantifying this change in wavelength have relied on measuring half-wavelengths along the body from video, based on the original methods described by Jayne (1985). These methods, while effective, can be time-consuming in practice (Gillis, 1998) and do not explicitly treat the kinematics of the snake between frames as dependent on one another with respect to time.

In this paper we measure the kinematics of swimming garter snakes and use non-linear regression techniques directly on the kinematic data to fit both a model in which the wavelength is held constant and a model in which the wavelength is permitted

☆ Presented as part of the Russell V. Baudinette Memorial Symposium held in Adelaide, Australia, 1-2 October 2005.

* Tel.: +1 510 643 9048; fax: +1 510 643-6264.
E-mail address: yonatanmunk@berkeley.edu.

1095-6433/$ - see front matter © 2007 Elsevier Inc. All rights reserved.
doi:10.1016/j.cbpa.2007.09.003

to vary exponentially along the length of the body. We then use statistical tests to determine whether the fit of the model to the data is significantly improved through the addition of a wavelength growth parameter.

In Jayne's original analysis, a significant correlation between propulsive wave frequency and swimming speed was found, and a slight decrease in amplitude and wavelength were noted as swimming speed increased. Using a more advanced digitization method, we hoped to further investigate the correlations between waveform parameters and swimming speed.

2. Materials and Methods

2.1. Animals

The kinematics in this study were obtained from four juvenile garter snakes (*Thamnophis sirtalis*; S1 length = 0.132 m, mass = 1.25 g; S2 length = 0.209 m, mass = 3.51 g; S3 length = 0.153 m, mass = 1.90 g; S4 length = 0.148 m, mass = 1.71 g), captured from various locations on the grounds of the Friday Harbor Laboratories (San Juan Island, Washington). In accordance with the animal care protocol obtained for this study, the snakes were not kept in the laboratory for more than a few hours before filming, and they were returned to their habitat immediately after completing their trials.

2.2. Procedures

The snakes were filmed while swimming in a still water tank with dimensions 1250 × 250 × 250 mm. Swimming was elicited by placing a given individual by hand at one end of the tank; upon release, the snakes tended to swim quite readily towards the opposite end of the tank. The snakes were not coerced to swim at specific speeds, but were permitted to choose their swimming speeds. A matte white bounce board inclined at 45 degrees was placed beneath the tank and illuminated with two 300 W halogen floodlights, providing a diffuse, even light source beneath the swimming animal. The animals were filmed from above at 250 fps with a Redlake MotionPro 10000 digital video camera at a resolution of 1280 × 960 pixels. Swimming bouts were only kept if the animal was swimming in the center of the tank and away from all walls. Typical swimming bouts consisted of approximately 4 to 8 tail beats, which were then divided into single tail beat sequences for analysis.

2.3. Digitization

The midline kinematics of the swimming snakes were obtained automatically via a custom Matlab 7.1 program. The video files were processed to provide extremely high contrast frames in which the swimming animal was silhouetted against a white background. The tracking algorithm, starting at the tip of the animal's skull in each frame, defined a half circle with radius equal to an initial segment length guess oriented so that the perimeter of the circle overlapped the body of the snake posterior to the rostrum. The next midpoint coordinate was placed at the point on the perimeter of this half circle corresponding to the middle region of the dark pixels detected along that perimeter (all dark pixels were assumed to be part of the snake's body). A new half-circle was then defined centered around this new midpoint coordinate, and this process continued until the tracking algorithm reached the end of the animal (i.e. found no more dark pixels).

The length of all segments laid out in this first pass along the animal were then summed and multiplied by the initial segment length guess to provide the length of the animal in pixels for that frame. This value was then multiplied by 0.95 and divided by 49 to provide the new optimum segment length for the tracking algorithm. The process was then run a second time, so that 50 equidistant points would be laid out along the anterior 95% of the animal's length. The final 5% of the animal was omitted from tracking since the cross-sectional area of this region was so small as to render its potential hydrodynamic contribution irrelevant; furthermore, it was observed that the tail tip frequently flicked out of the water or disrupted the surface of the water, leading to video artifacts which adversely affected the tracking algorithm.

This two-pass methodology was used to correct for first order errors of perspective in the video, as well as provide a means of checking for any vertical movements of the animal in the water column.

2.4. Statistics

To verify that the animal was swimming steadily in a given tailbeat sequence, we began by estimating the center of mass of the animal as the center of geometry of the 21 midline coordinates that were laid out along the thickest part of the trunk (points 10—30). The velocity of the center of mass was then calculated for the tail beat sequence and regressed against time. If the linear regression indicated that there was a significant increase in the center of mass velocity — judged as a greater than 10% change in trend line velocity over the course of a tail beat — the tail beat was deemed to be non-steady state.

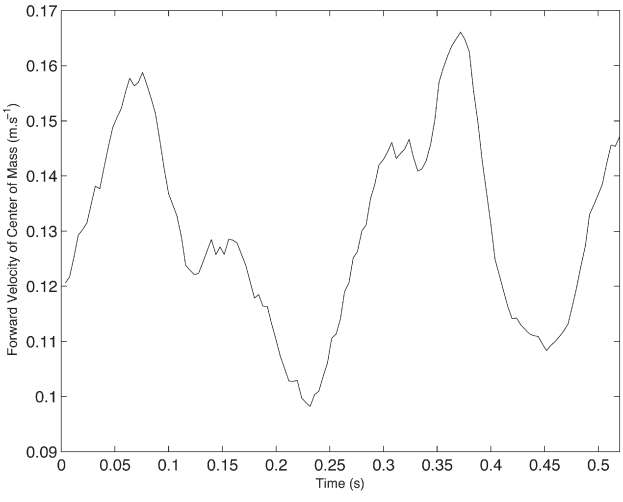

Fig. 1. Plot of the forward velocity of the center of mass in a representative 'steady swimming' sequence.

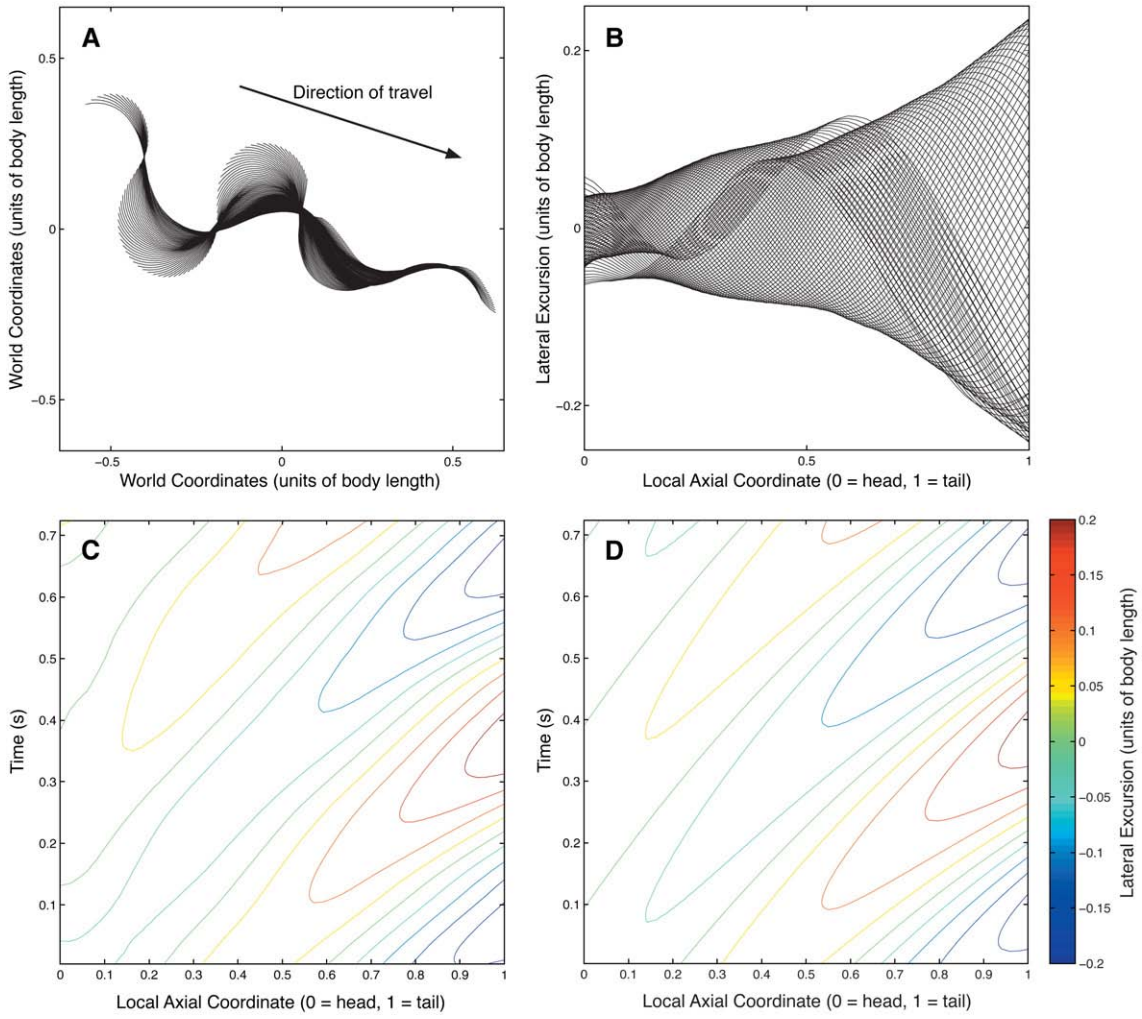

Fig. 2. (A) Digitized kinematics from a video segment containing a single full tail beat. Each individual line represents the midline of the snake in a given frame. [body length for this snake = 0.153 m] (B) The midlines from (A), following a coordinate transform whereby the *x*-coordinate is a relative body coordinate measuring the distance along the body of the animal from the head, and the *y*-coordinate is the lateral distance of the body at that point from the overall mean linear trajectory of the swimming animal (defined as the line $y=0$). (C) We can show the same information in (B) by creating a contour map whereby the vertical axis now represents time. In this figure the points of maximum displacement from the trajectory, traveling backwards along the animal, are represented as ridges on the contour map. The curvature evident in the shapes of these ridges is indicative of the non-constant propagation speed of the traveling wave. (D) For comparison, the contour map generated by the model described in Eq.(3) when fit to the data.

For all sequences, a linear regression was performed on the midline in each frame in a particular tail beat sequence, and the mean regression slope was used to approximate the overall linear trajectory of the animal for that tail beat. The data were rotated so that this overall trajectory became coincident with the *x*-axis and transformed so that the mean *y*-value for the entire dataset was 0.

The data were then treated as a 3-dimensional surface where the *x*-axis corresponded to the body coordinate (or distance from the head along the body), the *y*-axis corresponded to the frame number, and the *z*-axis corresponded to the lateral excursion of the midline of the animal from the overall linear trajectory. We then tested how well this surface was fit by several variants of the traveling wave equation, the simplest form of which is shown in Eq. (1).

$$z(s,t) = A\sin\left(2\pi\left(\frac{S}{\lambda} - ft\right)\right) \quad (1)$$

where s is the body coordinate, or node index, A is the amplitude, λ is the wavelength, f is the frequency of the oscillation, and t is the time, represented by the frame number. Two variations on Eq. (1) were considered in fitting a non-linear least squares regression to the data: one where only A was permitted to vary exponentially with s (following Tytell (2004b)), as shown in Eq. (2), and the other where both A and λ were permitted to vary with s, as shown in Eq.(3). An exponential change in body wavelength was chosen for Eq.(3) for symmetry with the exponential amplitude growth function, reflecting a presupposition that the growth in wavelength and in amplitude are related.

$$z(s,t) = Ae^{\alpha(s/L)}\sin\left(2\pi\left(\frac{S}{\lambda} - ft\right)\right) \quad (2)$$

$$z(s,t) = Ae^{\alpha(s/L)}\sin\left(2\pi\left(\frac{S}{\lambda e^{\gamma(s/L)}} - ft\right)\right) \quad (3)$$

where L is the total length of the animal, α is the amplitude growth rate and γ is the wavelength growth rate. These equations were fit to the data using nonlinear least squares regression. The benefit of this method is that parameters were estimated using all of the midline data from a sequence, rather than estimating these parameters from individual frames. Thus, the estimated parameters are the best fit parameters for the snake in a sequence given all of the available data.

2.5. Kinematic Correlations with Swimming speed

Using the parameter estimates for A, α, λ, γ and f from each tail beat sequence, a multiple regression over the entire dataset was performed to investigate the correlation of the model parameters with the observed swimming speed. Swimming speed for a given tail beat was calculated as the mean magnitude of the speed of the center of geometry of the midline over the entire course of the tail beat. The functional form of the multiple linear regression was as follows:

$$v = \beta_0 + \beta_1 A + \beta_2 \alpha + \beta_3 \lambda + \beta_4 \gamma + \beta_5 f \quad (4)$$

3. Results

After testing for acceleration in 101 tail beat sequences, 38 sequences exhibited a less than 10% change in the mean velocity of the center of mass over the course of the tail beat. It is important to note that the movements of the snakes involved characteristic oscillations with frequency equal to the tail beat frequency in the forward velocity of the center of mass — see Fig. 1. Steady swimming was judged on the basis of whether the oscillations in the forward speed of the center of mass exhibited a general trend with respect to time, as described in the Methods section. Furthermore, the amplitude of the undulatory wave did not approach zero towards the head, as is typically seen in other anguilliform swimmers.

Fig. 2 shows the kinematic data and model for a single tail beat from a representative video sequence (A), and that same data when rotated and transformed into body coordinates. This renormalized data is presented in two forms: one where all of the midlines from all frames are superimposed on one another (B), and the other where the same data is rendered as a contour map with body coordinate and frame number as the two axes (C). Finally, the predicted values from the fitted model are presented in contour form for comparison (D).

Table 1
Distribution of measured waveform parameters in 38 steady tail beat sequences.

	v ($BL\ s^{-1}$)	A (BL)	β	λ (BL)	γ	f (Hz)
Min.	0.6830	0.02563	0.887	0.3884	0.1845	1.269
1st Qu.	0.9179	0.03542	1.377	0.5214	0.3363	1.837
Median	1.0760	0.04183	1.597	0.5374	0.3663	2.183
Mean	1.1620	0.04416	1.571	0.5481	0.3715	2.358
3rd Qu.	1.4130	0.05329	1.717	0.5629	0.4141	2.549
Max.	1.9000	0.07905	2.358	0.9055	0.5675	4.655

All dimensions of length were normalized to body length (BL).

Table 2
Estimates (by multiple linear regression) of the correlation between the kinematic parameters of the model functional form (Eq. (3)) and observed swimming speed

	Estimate	Std. Error	t value	Pr(>|t|)	
(Intercept)	−2.12860	0.52229	−4.076	0.000283	***
A	26.59157	6.42111	4.141	0.000235	***
α	0.85016	0.28359	2.998	0.005224	**
λ	−0.31879	0.67297	−0.474	0.638920	
γ	−0.29119	0.69911	−0.417	0.679813	
F	0.45119	0.03695	12.211	1.38e-13	***

In all of the tail beat sequences analyzed, significantly non-zero parameter estimates were obtained for both the amplitude growth (α) and the wavelength growth (γ) parameters featured in Eq.(3). Between individuals, 1-way ANOVA tests conducted on each of the measured parameters failed to detect significant differences between individuals in all parameters aside from amplitude growth (α), although it should be noted that the statistical power of the ANOVA conducted on such a small sample size is low.

Within individuals, restricted vs. full F-tests unanimously indicated ($p<0.001$) that the addition of the wavelength growth parameter significantly improved the fit of the model beyond what would be expected by mere addition of an extra parameter to the functional form. The residuals tended to be larger for body coordinates approximately posterior to the anal vent, indicating that the motion of this region of the animal fits the functional form less well than the main trunk region.

A summary of the waveform parameters exhibited by steadily swimming snakes in this analysis is presented in Table 1. Table 2 shows the results of the multiple linear regression of swimming speed against the model parameters. The estimated coefficients for the head amplitude A, amplitude growth parameter α and the frequency f were all found to be significantly and positively correlated with swimming speed. The value for this full model was 0.84.

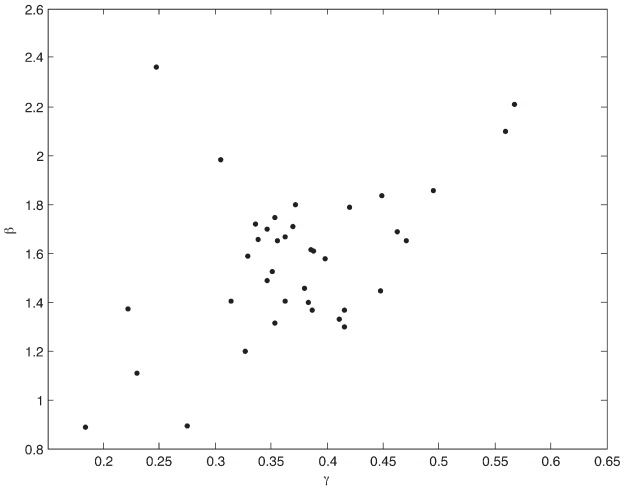

Fig. 3. Plot of amplitude growth parameter (λ) against the wavelength growth parameter (γ). In the steady swimming sequences analyzed, these were found to be strongly correlated with one another ($p<0.005$).

Furthermore, the amplitude growth parameter and the wavelength growth parameter were strongly correlated with one another ($p<0.005$); see Fig. 3.

4. Discussion

The results of our analysis concur with those of Jayne (1985) in finding that the kinematics of swimming snakes are well approximated by a undulatory model that exhibits an increasing wavelength and constant frequency, characteristics which have been shown to be shared by other anguilliform swimmers (Gillis, 1997, 1998). The non-linear regression method used in this experiment has allowed the comparison of models featuring constant wavelength and models featuring variable wavelength, and allows us to perform a restricted vs. full F-test on the two models to quantitatively assess the statistical merit of the addition of a wavelength growth parameter. In all tail beat sequences analyzed, including those that were not judged to be steady state, the model featuring non-constant wavelength was found to be a conclusively better fit than the constant wavelength model, providing statistical support for this previously observed (Jayne, 1985; Graham et al., 1987; Gillis, 1997, 1998) phenomenon.

The mean value for the wavelength growth parameter measured in steady swimming sequences was 0.37, implying that on average the wavelength at the tail of the animal was 1.5 times the wavelength at the head. As the frequency of undulation remained constant at all points along the body, this implies that the speed of propagation of the propulsive wave increased, on average, by a factor of 1.5 from head to tail.

Furthermore, it was found that the wavelength growth parameter was strongly correlated with the amplitude growth parameter; that is, snakes exhibiting large increases in undulatory amplitude from head to tail simultaneously exhibited a corresponding increase in wavelength along the body.

It should be noted that the definition of 'steady swimming' in this analysis is unusual, in the forward velocity of the center of mass of the animals was found to oscillate in a characteristic manner in all sequences analyzed — see Fig. 1. We defined steady swimming on the basis of whether a linear trend line fit to the center of mass velocity data plotted against time showed a significant slope, with steady swimming being identified as a change in center of mass velocity, judged using the fit trend line, of less than 10% over the course of a tail beat. This characteristic oscillation of center of mass velocity observed in the swimming snakes in this analysis has not been previously noted for other snakes, and that this does not appear to be exhibited in eels. This should be borne in mind when comparing the kinematics presented in this study for snakes with those of anguilliform swimmers capable of true steady swimming. Work by Tytell (2004a) has shown that accelerations can have significant impact on swimming kinematics, and the steady swimmers in this analysis are in fact undergoing regular accelerations and decelerations.

Using our criteria for steady swimming, 38 steady swimming tail beat videos were identified within the overall data set and a multiple linear regression was used to attempt to identify kinematic correlates between waveform parameters and swimming speed. Our results indicated that swimming speed was strongly correlated with undulatory frequency, and that swimming speed was also positively correlated with the amplitude at the head and the amplitude growth parameter. It should be noted that this is contrary to the previous findings of Jayne (1985), who reported an inverse correlation between swimming speed and relative amplitude. However, the low sample size of our analysis renders us hesitant to make any definitive statements in this regard. No correlation was found between wavelength or the wavelength growth parameter and swimming speed.

Acknowledgements

It was my great privilege to be the last student of the late R.V. Baudinette. His enthusiasm and support were instrumental in developing my desire to pursue science as a career. I would also like to thank T. Owerkowicz for organizing the symposium. S. Revzen, M. Koehl and the Berkeley biomechanics group provided many helpful comments during the preparation of this manuscript. The trenchant insights provided by two anonymous reviewers substantially improved the quality of the final manuscript. J. Horton and P. Domenici provided assistance and equipment for obtaining the kinematics. The research conducted was made possible by a scholarship awarded by the Friday Harbor Labs and a Ralph I. Smith memorial award from U.C. Berkeley.

References

Blake, R.W., 1983. Fish Locomotion. Cambridge University Press.
Gillis, G.B., 1996. Undulatory locomotion in elongate aquatic vertebrates: anguilliform swimming since Sir James Gray. Am. Zool. 36, 656–665.
Gillis, G.B., 1997. Anguilliform propulsion in an elongate salamander (Siren intermedia): Effects of speed on axial undulatory movements. J. Exp. Biol. 200, 767–784.
Gillis, G.B., 1998. Environmental effects on undulatory locomotion in the American eel Anguilla rostrata: kinematics in water and on land. J. Exp. Biol. 201, 949–961.
Graham, J.B., Lowell, W.R., Rubinoff, I., Motta, J., 1987. Surface and subsurface swimming of the sea snake Pelamis platurus. J. Exp. Biol. 27–44.
Gray, J., 1933. Studies in animal locomotion. I. The movement of fish with special reference to the eel. J. Exp. Biol. 10, 88–104.
Hertel, H., 1966. Structure – Form – Movement. Reinhold Publishing Corporation.
Jayne, B.C., 1985. Swimming in constricting (Elaphe g. guttata) and nonconstricting (Nerodia fasciata pictiventrus) colubrid snakes. Copeia 195–208.
Jordan, C.E., 1996. Coupling internal and external mechanics to predict swimming behavior: A general approach. Am. Zool. 36, 710–722.
Lighthill, J., 1969. Hydromechanics of aquatic animal propulsion. Annu. Rev. Fluid Mech. 1, 413–445.
Lighthill, J., 1971. Large-amplitude elongated-body theory of fish locomotion. Proc. Royal Soc. B 179, 125–138.
Lighthill, Sir James, 1975. Mathematical biofluiddynamics. Society for Industrial and Applied Mathematics.
Taylor, G.I., 1952. Analysis of the swimming of long and narrow animals. Proc. Royal Soc. A 241, 158–183.
Tytell, E.D., 2004a. Kinematics and hydrodynamics of linear acceleration in eels, Anguilla rostrata. Proc. Royal Soc., B, 271, 2535–2540.
Tytell, E.D., 2004b. The hydrodynamics of eel swimming II. Effect of swimming speed. J. Exp. Biol. 207, 3265–3279.
Tytell, E.D., Lauder, G.V., 2004. The hydrodynamics of eel swimming I. Wake structure. J. Exp. Biol. 207, 1825–1841.
Videler, J.J., Hess, F., 1984. Fast continuous swimming of two pelagic predators, saithe (Pollachius virens) and mackerel (Scomber scombrus): A kinematic analysis. J. Exp. Biol. 109, 209–228.